XVII IMEKO WORLD CONGRESS
Metrology for a Sustainable Development
September, 17–22, 2006 Rio de Janeiro, Brazil

ACCURATE PREDICTION OF ANALOG-TO-DIGITAL CONVERTER PERFORMANCE AFTER POST-CORRECTION

Henrik Lundin[1], *Peter Händel*[2], *Mikael Skoglund*[2]

[1] Global IP Sound, Stockholm, Sweden, hlu@kth.se
[2] KTH Electrical Engineering, Royal Institute of Technology, Stockholm, Sweden, ph@kth.se

Abstract: Analog-to-digital converter additive post-correction using look-up-tables is considered. An accurate expression is provided that predicts the ADC performance after correction. The expression depends on differential non-linearity, random noise variance, and the numerical precision of the correction terms. The theory shows good agreement when compared with simulations and experimental converter data.

Keyword: ADC, post-correction, look-up table, fixed-point, DNL.

1. INTRODUCTION

Analog-to-digital converter (ADC) post-correction has been proposed in many different forms, many of these applying look-up tables (LUTs) [1]. When designing ADC post-correction systems, it is of great interest to predict what performance that can be anticipated. The performance will, naturally, depend on the characteristics of the ADC at hand. Furthermore, in a practical post-correction application it is very likely that the correction values will be stored with fixed-point precision, which of course affects the corrected output. We will in this paper present a theory linking the ADC performance after post-correction with a number of design parameters. In particular, an expression for the signal-to-noise and distortion ratio will be provided. The theory is verified by computer simulations as well as experiments using a state-of-the-art ADC.

The work in the present paper is a continuation of the work in [2]. The theories below have been refined and expanded from [2], now also accounting for the characteristics of the converter nonidealities and random noise effects, improving the accuracy of the performance prediction. The presentation here is intentionally brief—the full derivations and further results and discussions are found in [3].

2. QUANTIZER AND CORRECTION SYSTEM MODEL

Consider an ADC with continuous-time input $s(t)$ and discrete-time output $x(n)$, as depicted in Fig. 1. The ADC is assumed to possess an ideal sample-and-hold circuit. Thus, the sampled signal $s(n)$ is regarded as input to the system. The quantizer has b bits, resulting in $M = 2^b$ quantization levels. The quantizer output, denoted $x(n)$, is a quantized version of $s(n)$. The quantization is defined by $M = 2^b$ disjunct regions $\mathscr{S}_0$ through $\mathscr{S}_{M-1}$, which together covers the entire input range. Each quantization region $\mathscr{S}_i$ is associated with

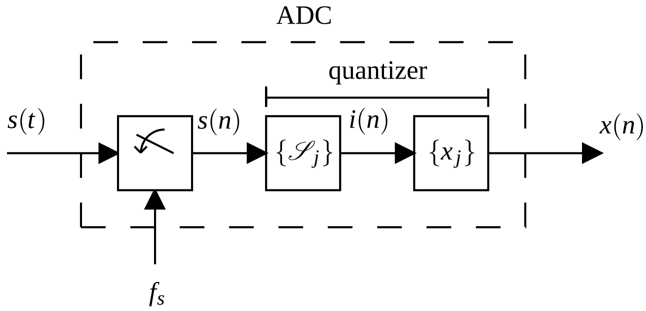

Fig. 1: A model for the ADC converter with the quantization represented as a two-step operation.

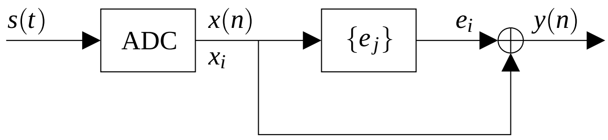

Fig. 2: Additive correction system.

one output level x_i which is assumed to be fixed but otherwise arbitrary. The quantization is defined such that $x(n) = x_i$ if $s(n) \in \mathscr{S}_i$. Also, the width of a quantization region is denoted the code bin width.

It is assumed that the input value $s(n)$ is drawn from a stochastic variable S with probability density function (PDF) $f_S(s)$. The temporal properties for S are immaterial since the quantizer is assumed to be non-dynamic, i.e., the output of the quantizer at time n depends only on the input at the same instant.

2.1 Post-correction System

A static additive correction (described for instance in [4]) is employed. Fig. 2 depicts the correction system. The corrected value y is produced by adding a correction term $e(x)$ to the output x so that $y = x + e(x)$. Every possible output value $x \in \{x_j\}_{j=0}^{M-1}$ is associated with a correction term $e(x) \in \{e_j\}_{j=0}^{M-1}$.

Optimal correction values for minimizing the mean-square error $\mathrm{E}[(S-y)^2]$ are used (note that y is a function of S and that the expectation is w.r.t. S). In [5] the minimum-mean-squared-error (MMSE) optimal correction values were derived. The result is that if the quantization regions $\{\mathscr{S}_j\}$

are assumed fixed, the optimal correction values are given by

$$\begin{aligned} e_{j,\text{opt}} &= \arg\min_y \mathrm{E}[(y-S)^2 | S \in \mathscr{S}_j] \\ &= \frac{\int_{s\in\mathscr{S}_j} s\, f_S(s)\, ds}{\int_{s\in\mathscr{S}_j} f_S(s)\, ds} - x_j. \end{aligned} \tag{1}$$

This is the correction that would be used if the correction values could be represented using infinite precision.

2.2 Mean Squared Error Calculations

Let MSE_Q denote the mean squared error (MSE) for the quantizer without correction, i.e.,

$$\begin{aligned} \text{MSE}_Q &= \mathrm{E}[(S-x)^2] = \int (s - \mathrm{Q}(s))^2\, f_S(s)\, ds \\ &= \sum_i \int_{s\in\mathscr{S}_i} (s-x_i)^2\, f_S(s)\, ds. \end{aligned} \tag{2}$$

The resulting MSE after infinite-precision correction – that is, applying correction terms according to (1) – is

$$\begin{aligned} \text{MSE}_o &= \mathrm{E}[(S-y)^2] = \mathrm{E}\left[(S-x)^2 - 2(S-x)\,e(x) + e(x)^2\right] \\ &= \text{MSE}_Q + \mathrm{E}\left[e(\mathrm{Q}(S))^2\right] - 2\,\mathrm{E}\left[(S-\mathrm{Q}(S))\,e(\mathrm{Q}(S))\right], \end{aligned} \tag{3}$$

where the last equality comes from applying (2). In order to simplify the expression, we use (1) to obtain

$$\int_{s\in\mathscr{S}_i} s\, f_S(s)\, ds = (e_i + x_i) \int_{s\in\mathscr{S}_i} f_S(s)\, ds, \tag{4}$$

and use it to manipulate the last term of the expression (3) into

$$\mathrm{E}[(S-\mathrm{Q}(S))\,e(\mathrm{Q}(S))] = \mathrm{E}\left[e(\mathrm{Q}(S))^2\right], \tag{5}$$

which is in fact nothing but the variance of the correction value e. Reapplying this in (3) yields

$$\text{MSE}_o = \text{MSE}_Q - \mathrm{E}\left[e(\mathrm{Q}(S))^2\right]. \tag{6}$$

Since $\mathrm{E}\left[e(\mathrm{Q}(S))^2\right]$ always is a non-negative quantity, we can immediately see that the MSE after MMSE-optimal correction is never higher than the MSE before correction, or $\text{MSE}_o \le \text{MSE}_Q$.

In the next section we will derive a more specific expression for the resulting MSE after correction based on certain assumptions on the quantizer behavior.

3. OPTIMAL CORRECTION RESULTS UNDER RANDOM DNL

In this section we will pursue a limit on how good a quantizer can be after correction. The nonidealities of the quantizer in terms of the differential nonlinearity (DNL) [6] are modeled as random. The maximum achievable MSE after MMSE optimal correction is derived and found to be dependent on the variance of the DNL process. The problem considered in this section was also studied in [7], and similar results as (17) were found then, but under different assumptions.

Assume that the ADC, or quantizer, suffers from a certain differential nonlinearity. We will here describe the DNL statistically in the following way. The ideal code bin width of the quantizer is denoted Δ. The actual code bin width for the k-th code bin is

$$W[k] = \Delta + d_\Delta[k]. \tag{7}$$

The DNL naturally becomes $\text{DNL}_k = d_\Delta[k]/\Delta$ in accordance with [6]. The differences $d_\Delta[k]$, $k = 1, 2, \ldots, M-2$, are considered to be independent realizations of a stochastic variable D with probability density function $f_D(d)$. It is assumed that $f_D(d)$ is an even function – implying zero-mean for D – and that the variance of D is σ_D^2.

The quantizer is still fed with a signal modeled as a stochastic variable S, with a PDF $f_S(s)$. The MSE is written as

$$\begin{aligned} \text{MSE} &= \mathrm{E}_S[(S-y)^2] = \int (s-y)^2\, f_S(s)\, ds \\ &= \sum_{k=0}^{M-1} \int_{\mathscr{S}_k} (s-y_k)^2\, f_S(s)\, ds \triangleq \sum_{k=0}^{M-1} \text{MSE}(k), \end{aligned} \tag{8}$$

where y_k is the corrected output for the k-th level: $y_k = x_k + e_k$. The mean-squared error in the k-th quantization region $\mathscr{S}_k$ as a function of $d_\Delta[k]$ is then

$$\begin{aligned} \text{MSE}(k; d_\Delta[k]) &= \mathrm{E}_S[(S-y_k)^2 | S \in \mathscr{S}_k; d_\Delta[k]] \\ &= \int_{\mathscr{S}_k} (s-y_k)^2\, f_S(s)\, ds. \end{aligned} \tag{9}$$

Note that the dependence on $d_\Delta[k]$ is in $\mathscr{S}_k$. Assume that the quantization region $\mathscr{S}_k$ is sufficiently small, and that $f_S(s)$ is sufficiently smooth, so that $f_S(s)$ can be considered a constant C_k within $\mathscr{S}_k$. Then, the MSE becomes

$$\text{MSE}(k; d_\Delta[k]) = C_k \int_{\mathscr{S}_k} (s-y_k)^2\, ds. \tag{10}$$

We also know (from (1)) in this case that the MMSE-optimal y_k is the midpoint of $\mathscr{S}_k$. With the substitution $t = s - y_k$ the integral can be written as

$$\text{MSE}(k; d_\Delta[k]) = 2C_k \int_0^{\frac{\Delta + d_\Delta[k]}{2}} t^2\, dt = \frac{C_k}{12}\,(\Delta + d_\Delta[k])^3. \tag{11}$$

By taking the expected value of $\text{MSE}(k; D)$ with respect to D, the MSE for the k-th quantization region is:

$$\begin{aligned} \text{MSE}(k) &= \mathrm{E}_D\left[\text{MSE}(k; D)\right] = \mathrm{E}_D\left[\frac{C_k}{12}\,(\Delta + D)^3\right] \\ &= \frac{C_k}{12}\left(1 + 3\frac{\sigma_D^2}{\Delta^2}\right)\Delta^3. \end{aligned} \tag{12}$$

The fact that D is zero-mean and that $\mathrm{E}[D^3] = 0$, since $f_D(d)$ is even, was used in the last equality. Upon inserting this into (8) the overall MSE is obtained as

$$\text{MSE}(\sigma_D^2) = \frac{\Delta^3}{12}\left(1 + 3\frac{\sigma_D^2}{\Delta^2}\right)\sum_{k=0}^{M-1} C_k. \tag{13}$$

It is perhaps more interesting to consider the relative MSE. In particular, we consider the MSE related to the MSE for an ideal quantizer, fed with the same signal. The MSE for an ideal quantizer, denoted MSE_Q as before, was expressed in (2). By making the smoothness assumption again, the ideal MSE can be approximated as

$$\begin{aligned} \mathrm{MSE}_Q &= \sum_{k=0}^{M-1} \int_{s\in\mathscr{S}_k'} (s-x_k)^2 \, f_S(s)\, ds \\ &\approx 2\sum_{k=0}^{M-1} C_k' \int_0^{\frac{\Delta}{2}} t^2\, dt = \frac{\Delta^3}{12}\sum_{k=0}^{M-1} C_k', \end{aligned} \tag{14}$$

where $'$ is used to denote that $\mathscr{S}_k'$ and C_k' are not necessarily equal to $\mathscr{S}_k$ and C_k, respectively. The potential discrepancy between $\mathscr{S}_k'$ and $\mathscr{S}_k$ does of course come from the deviation $d_\Delta[k]$ in the regions. Since the regions may end up at different places, the assumed constant value C_k' for the PDF $f_S(s)$ may consequently change to C_k.

Define the ratio between $\mathrm{MSE}(\sigma_D^2)$ and MSE_Q as

$$\kappa \triangleq \frac{\mathrm{MSE}(\sigma_D^2)}{\mathrm{MSE}_Q} = \frac{\frac{\Delta^3}{12}\left(1+3\frac{\sigma_D^2}{\Delta^2}\right)\sum_{k=0}^{M-1} C_k}{\frac{\Delta^3}{12}\sum_{k=0}^{M-1} C_k'}. \tag{15}$$

The assumption that

$$\sum_{k=0}^{M-1} C_k \approx \sum_{k=0}^{M-1} C_k' \tag{16}$$

is rather reasonable—multiplying each sum by Δ gives an approximation of the integral $\int f_S(s)\, ds = 1$. Under that assumption, κ simplifies to

$$\kappa \approx \left(1+3\frac{\sigma_D^2}{\Delta^2}\right). \tag{17}$$

This is the increase in MSE that is inflicted by the DNL *after* MMSE optimal correction is applied.

3.1 SINAD and ENOB

The result (17) above can be directly translated to a degradation in the signal-to-noise and distiortion ratio (SINAD), and the effective number of bits (ENOB). The SINAD is defined as [6]

$$\mathrm{SINAD} = 20\log_{10}\frac{\mathrm{RMS}_{\mathrm{signal}}}{\mathrm{RMS}_{\mathrm{noise}}}, \tag{18}$$

where we can use $\mathrm{RMS}_{\mathrm{noise}} = \sqrt{\mathrm{MSE}} = \sqrt{\kappa \mathrm{MSE}_Q}$. This is of course assuming that there are no other noise sources affecting the quantizer. Thus, the difference between the SINAD with optimally corrected DNL errors and the SINAD of an ideal converter is

$$\Delta\mathrm{SINAD} = -10\log_{10}\left(1+3\frac{\sigma_D^2}{\Delta^2}\right) \text{ dB}. \tag{19}$$

The ENOB is directly linked with the SINAD (cf. [6]), and we can therefore state the difference between the ENOB with DNL errors and the ENOB of an ideal converter as

$$\Delta\mathrm{ENOB} = -\frac{1}{2}\log_2\left(1+3\frac{\sigma_D^2}{\Delta^2}\right) \text{ bits}, \tag{20}$$

again provided that the errors are corrected using (1).

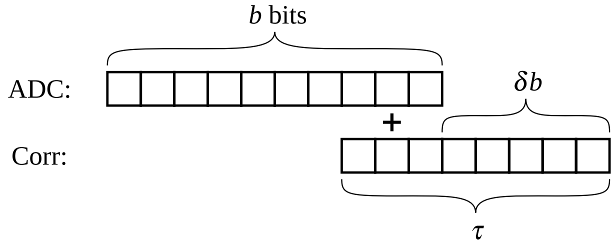

Fig. 3: Addition of the ADC output with a correction value. The bits of the table value are shifted in order to enhance the precision of the corrected ADC.

4. FIXED-POINT RESOLUTION FOR CORRECTION VALUES

It is not always feasible, let alone practical, to implement an ADC post-correction system, such as the one in Fig. 2, using floating-point[1] representation for the stored correction values $\{e_j\}_{j=0}^{M-1}$. It is natural to settle for a specific precision with which the correction terms are stored, e.g., a certain number of bits. Obviously, the performance of the corrected ADC will depend on which precision that is used to store the correction values.

The precision of digitally stored values is often stated as a number of bits. Assume that the table is stored using τ bits and that the ADC to be corrected converts the signal into b-bit values. If we know that the ADC only has error in the lower bits, then we can "shift" the bits of the correction table and obtain a correction with higher effective precision. For example, if the ADC has 10 bits, but only the 2 LSBs need correction, then the remaining bits of the correction values (minus the sign bit) can be used to get a better precision.

After the correction with a shifted correction value we have an ADC with a b-bit resolution but a supra-b bit precision. That is, the ADC still has got 2^b quantization regions, but the reconstruction levels after correction are represented with more than b bits.

The problem gets easier to analyze if the resolution η, being the smallest possible difference between two different correction values, is used instead of the actual number of bits τ. Moreover, we are here only interested in the number of extra bits δb added by the correction term. See Fig. 3 for an illustration. The relationship between δb and η is straightforward:

$$\eta = 2^{-\delta b} \text{ LSBs}. \tag{21}$$

It is assumed that the correction values never exceed the largest number that can be represented by the τ correction bits, meaning that saturation of the correction values does not happen.

Let $\tilde{e}_i$ be the (uniformly) quantized version of the table entry e_i. This is the correction value that would be used in a post-correction system with a fixed-point resolution η. We assume that one of the quantization cells is centered at zero. That is, if a certain correction term is within the interval $[-\eta/2, \eta/2]$ it will be quantized to zero, and, since the quantization of correction terms is uniform (ideal round-off), all other possible quantized values are located at an integer multiple of η. Hence, we can say that

$$\tilde{e}_i \in \{k\eta : k = \ldots, -2, -1, 0, 1, 2, \ldots\}. \tag{22}$$

[1] Floating-point representation of numbers does not have infinite precision, but it is the closest to infinite precision we can muster in a digital implementation.

Also let

$$\delta_i = \tilde{e}_i - e_i \tag{23}$$

be the difference between the fixed-point and the infinite-precision correction terms. The notation $\delta(x)$ denotes the correction term quantization error associated with a specific x, i.e., $\delta(x) = \delta_i$ if $x = x_i$.

4.1 MSE

Once again we calculate the MSE of the corrected output signal. The MSE obtained using the quantized correction terms becomes

$$\begin{aligned}\mathrm{MSE}_\eta &\triangleq \mathrm{E}\left[(S - x - \tilde{e}(x))^2\right] = \mathrm{E}\left[(S - x - e(x) - \delta(x))^2\right] \\ &= \mathrm{MSE}_o + \mathrm{E}[\delta(x)^2] - 2\,\mathrm{E}[(S - x - e(x))\delta(x)].\end{aligned} \tag{24}$$

The error term $\delta(x)$ ultimately depends on the stochastic variable S. Using the (modified) relationship in (4), it is easy to show that $\mathrm{E}[(S - x - e(x))\,\delta(x)] = 0$, and we obtain

$$\mathrm{MSE}_\eta = \mathrm{MSE}_o + \mathrm{E}[\delta(x)^2]. \tag{25}$$

The second moment of the error $\mathrm{E}[\delta(x)^2]$ can further be written as

$$\begin{aligned}\mathrm{E}[\delta(x)^2] &= \int \delta(x)^2\, f_S(s)\, ds = \sum_i \int_{s \in \mathscr{S}_i} \delta_i^2\, f_S(s)\, ds \\ &= \sum_i \int_{s \in \mathscr{S}_i} f_S(s)\, ds \frac{\int_{s \in \mathscr{S}_i} \delta_i^2\, f_S(s)\, ds}{\int_{s \in \mathscr{S}_i} f_S(s)\, ds} \\ &= \sum_i \int_{s \in \mathscr{S}_i} f_S(s)\, ds\, \mathrm{E}[\delta^2 | S \in \mathscr{S}_i].\end{aligned} \tag{26}$$

Under the assumption that the quantization error δ_i is uniformly distributed in $[-\eta/2, \eta/2]$, then each $\mathrm{E}[\delta^2 | S \in \mathscr{S}_i] = \eta^2/12$ for all i, and (26) becomes

$$E[\delta(x)^2] = \frac{\eta^2}{12} \sum_i \int_{s \in \mathscr{S}_i} f_S(s)\, ds = \frac{\eta^2}{12}. \tag{27}$$

The MSE in (25) then boils down to

$$\mathrm{MSE}_\eta = \mathrm{MSE}_o + \frac{\eta^2}{12}. \tag{28}$$

Since η is expressed in LSBs, so should also MSE_o be. Alternatively, the second term can be scaled by Δ^2 to get the result in input units, e.g., V^2 (volts squared).

It is reasonable to believe that the assumption leading up to (27) is valid for small η, i.e., when the quantization is assumed to be "high-rate". (See [8] for a thorough discussion and precise conditions for the uniformity of the quantization noise.) However, as η grows large the assumption will become invalid, motivating the asymptotic analysis.

4.2 Asymptotic MSE

Recall that one of the quantization cells is centered at zero and that all table values e_i that fall within $[-\eta/2, \eta/2]$ will be quantized to $\tilde{e}_i = 0$. When we enlarge the correction value quantization step, i.e., when $\eta \to \infty$, all $\tilde{e}_i$ will inevitably be zero, since all table values will fall into the expanding center region at zero. Consequently, the resulting MSE becomes

$$\mathrm{MSE}_\eta = \mathrm{E}[(S - x - 0)^2] = \mathrm{E}[(S - x)^2] = \mathrm{MSE}_Q \tag{29}$$

when the resolution tends to zero. The interpretation is straightforward: since no correction is effected, the MSE is that of the uncorrected quantizer. The MSE will increase with η according to (28), but not any further than to MSE_Q.

5. RANDOM INPUT NOISE

Errors in the transfer function that are deterministic can be compensated for. The results of the previous sections show how successful this compensation is, taking the DNL of the quantizer and the precision of correction values into account. One error effect of a practical ADC that *cannot* be compensated for using look-up tables[2] is random noise. Since the noise is truly random, it is impossible to say anything about it, even with knowledge of the resulting output signal. Hence, it cannot be compensated for.

The random noise is modeled as an additive noise, with variance σ_n^2, added to the input of the quantizer. As a natural consequence, the MSE of the output is increased by σ_n^2.

6. COMBINING THE THEORIES

The performance description provided in (28) above is dependent on MSE_o – a quantity that is dependent on the actual transfer characteristics of the ADC under test, the accuracy of the calibration and correction schemes, and on the signal considered. One way to obtain MSE_o is of course to test it in practice – that is calibrate an infinite-precision LUT and use it to evaluate the resulting MSE after correction. This is, however, cumbersome in many situations. It would therefore be interesting to find an expression for MSE_o that could be used to estimate the resulting performance of a post-corrected ADC before it was calibrated.

In this section, the theories presented above are combined to form a joint formula for the resulting performance after correction, as a function of DNL, LUT resolution and random noise.

Recall from (15) that the MSE after correction using perfect (infinite-precision) correction values could be expressed as

$$\mathrm{MSE}(\sigma_D^2) = \kappa\,\mathrm{MSE}_Q = \left(1 + 3\frac{\sigma_D^2}{\Delta^2}\right)\mathrm{MSE}_Q. \tag{30}$$

Here, σ_D^2 was the variance of the DNL, and Δ was the nominal quantization bin width.

In order to get a value for MSE_Q – the error of an ideal quantizer – we make the assumption that the quantization step size Δ of the ADC is small compared with the variability of the source PDF and that the input signal does not overload the quantizer. Then, MSE_Q is the classical result

$$\mathrm{MSE}_Q = \mathrm{MSE}_{\text{uniform}} = \frac{\Delta^2}{12}. \tag{31}$$

Now, inserting (31) into (30), and this in turn into (28), gives the resulting MSE after correction with a fixed-point LUT. We also account for a random noise with variance σ_n^2 as in Sect. 5. The result is

$$\begin{aligned}\mathrm{MSE}_\eta(\sigma_D^2, \sigma_n^2) &= \left(1 + 3\frac{\sigma_D^2}{\Delta^2}\right)\frac{\Delta^2}{12} + \frac{\eta^2\Delta^2}{12} + \sigma_n^2 \\ &= \frac{\Delta^2}{12} + \frac{\sigma_D^2}{4} + \frac{\eta^2\Delta^2}{12} + \sigma_n^2.\end{aligned} \tag{32}$$

[2] Random noise can be compensated using oversampling and averaging techniques, but this limits the input frequency range.

The MSE consists of four terms: the first term is the MSE of the ideal uniform quantization, the second term is the error inflicted by the DNL, the third term is the effect of limited-resolution correction values, and the fourth term is the input random noise. Note that the result is in squared input units, e.g., V^2. The resulting MSE in LSB^2 is obtained simply by dividing the equation by Δ^2.

6.1 SINAD

When characterizing ADCs the SINAD, defined in (18), is more frequently used than the MSE. It is therefore interesting to state the result obtained above in terms of SINAD instead of MSE. The SINAD is in most cases tested using a sinewave signal. Let the amplitude of the test signal be A_{dBFS}, expressed in dB relative full scale. Hence, the RMS value is

$$\text{RMS}_{\text{signal}} = \frac{\Delta 10^{\frac{A_{\text{dBFS}}}{20}}\, 2^{b-1}}{\sqrt{2}}. \quad (33)$$

The RMS noise amplitude is obtained from the MSE expression (32) above so that

$$\text{RMS}_{\text{noise}} = \sqrt{\text{MSE}_{\eta}(\sigma_D^2, \sigma_n^2)}. \quad (34)$$

We obtain the expression

$$\begin{aligned}\widehat{\text{SINAD}} &= 20\, b \log_{10} 2 + 10 \log_{10} \frac{3}{2} + A_{\text{dBFS}} \\ &\quad - 10 \log_{10} \left(1 + 3\frac{\sigma_D^2}{\Delta^2} + \eta^2 + 12\frac{\sigma_n^2}{\Delta^2}\right)\end{aligned} \quad (35)$$

for the resulting SINAD in dB. Note that A_{dBFS} must be negative for this expression to be valid. If not, the quantizer is overdriven, and the MSE in (32) is no longer accurate.

6.2 ENOB

The ENOB is defined in [6] as a function of the SINAD. Straightforward calculations from (35) gives

$$\text{ENOB}_{\text{DNL}} = b - \frac{1}{2}\log_2\left(1 + 3\frac{\sigma_D^2}{\Delta^2} + \eta^2 + 12\frac{\sigma_n^2}{\Delta^2}\right). \quad (36)$$

7. SIMULATIONS

The results derived in the present paper have been tested in simulation experiments. In the experiment reported here, the model was a simple quantizer where the widths of the quantization regions were randomly altered from an ideal uniform configuration.The input signal was first perturbed by additive Gaussian noise, with zero mean and variance $\sigma_n^2 = 0.05$ LSB^2. The subsequent quantizer had a DNL that for each code level was generated as an independent observation of a zero-mean Gaussian random variable with variance $\sigma_D^2 = 0.002$ LSB^2. The resolution of the quantizer is $b = 10$ bits. The following steps are taken in the simulation:

1. Calibrate a LUT. A sinusoid with amplitude –1 dBFS and random initial phase is used as input to the ADC model. The normalized frequency (f/f_s) is selected to $3001/16384 \approx 0.1832$, i.e., the conditions for coherent sampling [6] are fulfilled for a record of 16 384 samples, which is the size of the record taken.

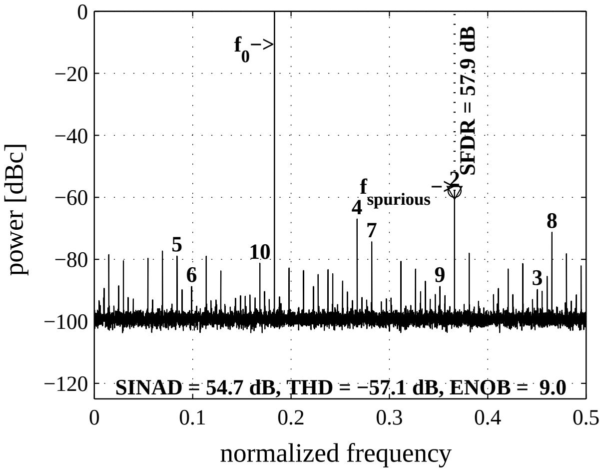

Fig. 4: The average output spectrum of the 16 test signals before correction.

2. A sinewave fit is made to the recorded data, as per the IEEE standard [6]. The fitted sinewave is used as reference signal and a correction table is built (cf. [4]). The correction table is static, i.e., having one correction term per ADC code level. The correction terms are stored in floating-point precision.
3. Evaluate the correction. 16 sinusoid test signals are generated, each having amplitude and frequency as above and random initial phase. These are used as input to the ADC model and the resulting output is corrected using the LUT. The performance in terms of mean SINAD over the 16 sequences is calculated.
4. The LUT correction values are quantized to lower precision η, and the evaluation step 3 is repeated for different values of η.

Fig. 4 shows the output spectrum of the uncorrected quantizer, evaluated using the 16 sinusoids in step 3. Fig. 5(a) shows the resulting SINAD after correction with varying precision η. The graph shows the simulation results ('o') together with the theoretical result $\widehat{\text{SINAD}}$ as predicted in (35) (solid line). The graph also shows two horizontal lines, where the upper ('△') shows the SINAD after correction with infinite precision, and the lower ('∇') shows the SINAD of the uncorrected ADC model.

We see from the results that the theoretical line $\widehat{\text{SINAD}}$ aligns well with the simulation results, up to $\delta b = 0$. For poorer resolution than that, i.e., for $\delta b < 0$ implying $\eta >$ 1 LSB, the experimental SINAD approaches that of the uncorrected ADC. This is in perfect accordance with the discussion in Sect. 4.2, where it was argued that the performance would not be worse than that of the uncorrected ADC. It does also make sense that a table resolution $\eta \geq 2$ LSBs does not provide much improvement, since the vast majority of the table values in this case had a magnitude less than 1.

8. RESULTS USING EXPERIMENTAL ADC DATA

The theories presented in the present paper have also been evaluated using experimental ADC data, acquired from an Analog Devices AD9430, 210 MSPS, 12 bit converter. The test equipment used was described in [9], and the aquired data is described in detail in [3, Appendix B.3].

From the measurements the following parameters were estimated:

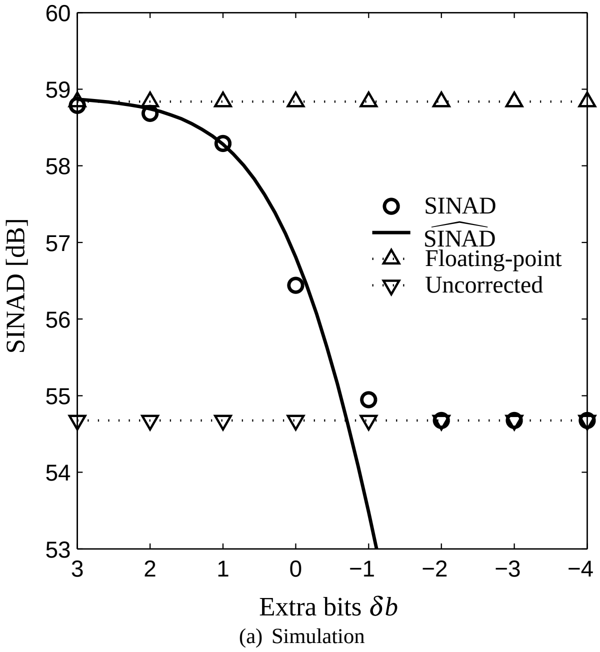

(a) Simulation

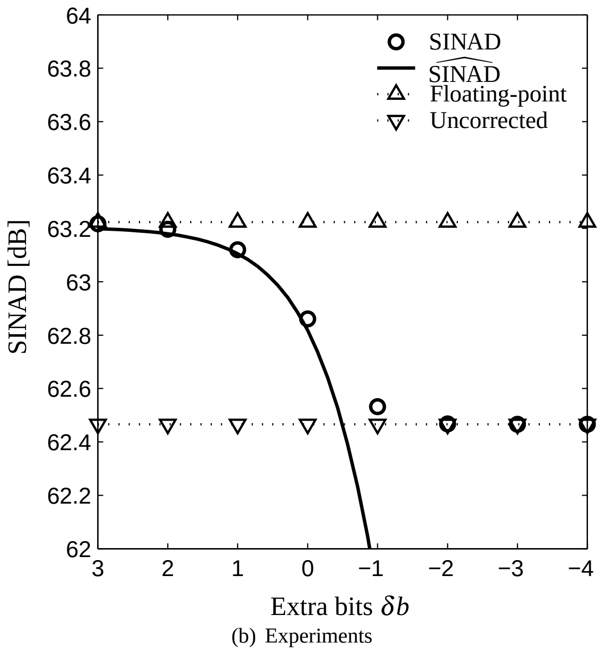

(b) Experiments

Fig. 5: Comparison between the theoretical expression $\widehat{\mathrm{SINAD}}$ (solid) and the results obtained through (a) simulations or (b) experimental data, both marked with 'o'. The top and bottom horizontal lines show the resulting SINAD after correction using floating-point precision ('$\triangle$') and no correction at all ('∇'), respectively. Note that the model used to obtain the results in (a) is not intended to describe the specific ADC used in (b), wherefore the results show a significant difference in scale between (a) and (b).

- Random noise variance: $\sigma_n^2 \approx 0.8092$ LSB^2.
- Variance of DNL: $\sigma_D^2 \approx 0.004206$ LSB^2.

With these values we can estimate the performance in terms of SINAD of the converter after correction using the formula (35).

An LUT is calibrated and used for correction. The procedure is quite similar to that used in the simulations of Sect. 7 with these modifications:

- The sinusoid amplitude is –0.5 dBFS.
- The signal frequency is 60 124 547 Hz and the sample rate is 209 993 728 Hz.
- The recorded data consists of sequences of 65 536 samples each.
- 31 sequences are used for LUT calibration, and another set of 31 seqeunces are used for evaluation.

Fig. 5(b) shows the results using the experimental ADC data. We see a good match between the experimental results and the predicted value from (35).

9. CONCLUSIONS

In this paper, we have presented a method to predict the performance of an ADC after MMSE-optimal additive static correction. The results provided equations for the resulting MSE, SINAD and ENOB after correction. The theories show how the intrinsic ADC parameters – resolution, DNL variance and random noise variance – and the resolution of the correction values all affect the fidelity of the output. The work presented herein is an improvement of the results of [2], now also taking DNL and random noise into account. The results were verified with computer simulations as well as using experimental ADC data.

REFERENCES

[1] Eulalia Balestrieri, Pasquale Daponte, and Sergio Rapuano. A state of the art on ADC error compensation methods. *IEEE Transactions on Instrumentation and Measurement*, 54(4):1388–1394, August 2005.

[2] Henrik Lundin, Mikael Skoglund, and Peter Händel. ADC post-correction using limited resolution correction values. In *Proceedings IMEKO 10th Workshop on ADC Modelling and Testing*, volume 2, pages 567–572, Gdynia/Jurata, Poland, September 2005.

[3] Henrik F. Lundin. *Characterization and Correction of Analog-to-Digital Converters*. PhD thesis, Royal Institute of Technology (KTH), November 2005. TRITA-S3-SB-0575. Available from: `http://www.ee.kth.se`.

[4] Peter Händel, Mikael Skoglund, and Mikael Pettersson. A calibration scheme for imperfect quantizers. *IEEE Transactions on Instrumentation and Measurement*, 49:1063–1068, October 2000.

[5] Stuart P. Lloyd. Least squares quantization in PCM. *IEEE Transactions on Information Theory*, IT-28(2):129–137, March 1982.

[6] IEEE. *IEEE Standard for Terminology and Test Methods for Analog-to-Digital Converters*. IEEE Std. 1241. 2000.

[7] Nicola Giaquinto, Mario Savino, and Amerigo Trotta. Detection, digital correction and global effect of A/D converters nonlinearities. In Pasquale Daponte and Linus Michaeli, editors, *International Workshop on ADC Modelling*, pages 122–127, Slovak Republic, May 1996. IMEKO.

[8] Bernard Widrow, István Kollár, and Ming-Chang Liu. Statistical theory of quantization. *IEEE Transactions on Instrumentation and Measurement*, 45(2):353–361, April 1996.

[9] Niclas Björsell and Peter Händel. High dynamic range test-bed for characterization of analog-to-digital converters. In *10th Workshop on ADC modelling and testing*, pages 601–604, Gdynia and Jurata, Poland, September 2005.